터널과 지하공간, 한국암반공학회
Vol. 9, 1999, pp. 149~157

TUNNEL & UNDERGROUND Vol. 9, 1999, pp. 149-157
J. of Korean Society for Rock Mech.

불연속 변형 해석법에 의한 지하수-암반블록 상호작용 모델링

김 용 일[1)]

Modeling the Water-Block Interaction with Discontinuous Deformation Analysis Method

Yong-Il Kim

ABSTRACT A powerful numerical method that can be used for that purpose is the Discontinuous Deformation Analysis (DDA) method developed by Shi in 1988. In this method, rock masses are treated as systems of finite and deformable blocks. Large rock mass deformations and block movements are allowed. Although various extensions of the DDA method have been proposed in the literature, the method is not capable of modeling water-block interaction that is needed when modeling surface or underground excavation in fractured rock. This paper presents a new extension to the DDA method. The extension consists of hydro-mechanical coupling between rock blocks and water flow in fractures. A example of application of the DDA method with the new extension is presented. The results of the present study indicate that fracture flow could have a destabilizing effect on the tunnel stability.

Key words : Discontinuous deformation analysis, Hydro-mechanical coupling, Fracture, Water flow, Tunnel stability

초 록 불연속 변형 해석법(Discontinuous Deformation Analysis Method)은 1988년에 Shi에 의해 개발되었으며, 암반-구조물 상호작용 모델링에 매우 효율적인 해석법이다. 이 해석법에서 암반은 유한하고 변형가능한 블록으로 간주되며, 암반의 대변형 및 이동이 가능하다. 그 후, DDA 방법에 대한 여러가지 보완사례가 발표되었으나, 균열이 발달한 암반의 지표 또는 지중 굴착 모델링에 긴요한 지하수-암반블록 상호작용 모델링은 불가능하다. 본 논문에서는 암반 블록 사이의 수리-역학적 커플링을 고려하기 위한 새로운 방법이 제시된다. 또한, 이 방법이 보완된 새로운 DDA 해석법의 적용 예가 제시된다. 본 연구결과 암반 균열 사이를 흐르는 지하수는 터널의 안정성에 나쁜 영향을 미친다는 사실이 확인되었다.

핵심어 : 불연속 변형 해석법, 수리-역학적 커플링, 균열, 지하수 흐름, 터널안정

1. Introduction

Several numerical methods are used in rock mechanics to model the response of rock masses to loading and unloading. These methods include the Finite Element Method(FEM), the Boundary Element Method(BEM) and the Discrete Element Method(DEM). Compared to the FEM and BEM methods, the DEM method is tailored for structurally controlled stability problems in which there are many material discontinuities and blocks. The DEM method allows for large deformations along discontinuities and can reproduce rock block translation and rotation quite well.

Shi and Goodman(1984) firstly presented the backward model of DDA method which can compute the strains and displacements of blocky systems from a set of displacements and strain measurement made at a sufficient number of points. Shi(1989) first proposed a new discontinuous deformation analysis(DDA) method consisting of backward and forward models in this doctoral thesis; computer programs based on the method were developed and some applications were presented in the thesis and various publications(Shi and Goodman 1989; Shi 1990; Ke and Goodman 1994; Yeung and Klein 1994).

Recently, Lin(1995) improved the original DDA program by Shi(1989) with four major extensions: improvement of block contact, calculation of stress distributions within blocks using sub-blocks, block

1) 정회원, (주)대우 건설기술연구소 선임연구원
원고 접수일 : 1999년 4월 19일
원고 심사 완료일 : 1999년 6월 18일

fracturing and viscoelastic behavior.

Besides the work of Lin(1995), various modifications to the original DDA formulation have been reported in the rock mechanics literature, in particular, in the proceedings of the First International Forum on DDA (Salami and Banks, 1996) and the 2nd International Conference on Analysis of Discontinuous Deformation (Ohnishi, 1997). But, the method still has many limitations when applied to many specific engineering problems. In this thesis, several major limitations of the DDA method are addressed. This paper presents new tools that have been developed and implemented into the original DDA method to solve these limitation.

In rock masses there are generally many discontinuities that are preferred pathways for groundwater. Water flow induces hydrostatic pressure and seepage forces that affect the state of stress in the rock masses. At the same time, changes in the state of stress induce rock mass deformation, which result in changes in the rock mass hydraulic properties. This hydro-mechanical coupling is critical and cannot be ignored when modeling rock-structure interaction in engineering problems where water is present.

2. Modeling Blocky Rock Masses in the DDA Method

In the DDA method, the formation of blocks is very similar to the definition of a finite element mesh. A finite element type of problem is solved in which all the elements are physically isolated blocks bounded by pre-existing discontinuities. The elements or blocks used by the DDA method can be of any convex or concave shape whereas the FEM method uses only elements with predetermined topologies. When blocks are in contact, Coulomb's law applies to the contact interfaces and the simultaneous equilibrium equations are selected and solved at each loading or time increment. The large displacements and deformations are the accumulation of small displacements and deformations at each time step. Within each time step, the displacements of all points are small, hence the displacements can be reasonably represented by first order approximations.

The DDA method has a number of features similar to the FEM. However, the main attraction of the DDA method is its capability of reproducing large deformations along discontinuities and large block movement; two features that are restricted with the FEM.

2.1 Block Deformations

By adopting first order displacement approximations, the DDA method assumes that each block has constant stresses and strains throughout. The displacements (u, v) at any point (x, y) in a block, i, can be related in two dimensions to six displacement variables

$$\mathbf{D}_i = (d_{1i}\ d_{2i}\ d_{3i}\ d_{4i}\ d_{5i}\ d_{6i})^T = (u_0\ v_0\ r_0\ \varepsilon_x\ \varepsilon_y\ \gamma_{xy})^T \quad (1)$$

where (u_0, v_0) is the rigid body translation at a specific point (x_0, y_0) within the block, r_0 is the rotation angle of the block with the rotation center at (x_0, y_0) and ε_x, ε_y and γ_{xy} are the normal and shear strains in the block. As shown by Shi(1988), the complete first order approximation of block displacements takes the following form

$$\begin{bmatrix} u \\ v \end{bmatrix} = \mathbf{T}_i \mathbf{D}_i \quad (2)$$

where

$$T_i = \begin{bmatrix} 1 & 0 & -(y-y_0) & (x-x_0) & 0 & (y-y_0)/2 \\ 0 & 1 & (x-x_0) & 0 & (y-y_0) & (x-x_0)/2 \end{bmatrix} \quad (3)$$

This equation enables the calculation of the displacements (u, v) at any point (x, y) within the block (in particular, at the corners), when the displacements are given at the center of rotation and when the strains (constant within the block) are known. In the two-dimensional formulation of the DDA method, the center of rotation with coordinates (x_0, y_0) coincides with the block centroid.

2.2 Simultaneous Equilibrium Equations

In the DDA method, individual blocks form a system of blocks through contacts among blocks and displacement constraints on single blocks. Assuming that n blocks are defined in the block system, Shi(1988) showed that the simultaneous equilibrium equations can be written in matrix form as follows

$$\begin{bmatrix} \mathbf{K}_{11} & \mathbf{K}_{12} & \mathbf{K}_{13} & \cdots & \mathbf{K}_{1n} \\ \mathbf{K}_{21} & \mathbf{K}_{22} & \mathbf{K}_{23} & \cdots & \mathbf{K}_{2n} \\ \mathbf{K}_{31} & \mathbf{K}_{32} & \mathbf{K}_{33} & \cdots & \mathbf{K}_{3n} \\ \vdots & \vdots & \vdots & \ddots & \vdots \\ \mathbf{K}_{n1} & \mathbf{K}_{n2} & \mathbf{K}_{n3} & \cdots & \mathbf{K}_{nn} \end{bmatrix} \begin{Bmatrix} \mathbf{D}_1 \\ \mathbf{D}_2 \\ \mathbf{D}_3 \\ \vdots \\ \mathbf{D}_n \end{Bmatrix} = \begin{Bmatrix} \mathbf{F}_1 \\ \mathbf{F}_2 \\ \mathbf{F}_3 \\ \vdots \\ \mathbf{F}_n \end{Bmatrix} \quad (4)$$

where each coefficient $\mathbf{K}_{ij}$ is defined by the contacts between blocks i and j. Since each block i has six degrees of freedom defined by the components of $\mathbf{D}_i$ in equation (1), each $\mathbf{K}_{ij}$ in equation (4) is itself a 6×6 sub-matrix. Also, each $\mathbf{F}_i$ is a 6×1 sub-matrix that represents the loading on block i. Equation (4) can also be expressed in a more compact form as **KD=F** where **K** is a 6n x 6n stiffness matrix and **D** and **F** are 6n× 1 displacement and force matrices, respectively. In total, the number of displacement unknowns is the sum of the degrees of freedom of all the blocks. It is noteworthy that the system of equations (4) is similar in form to that in finite element problems.

The solution to the system of equations (4) is constrained by a system of inequalities associated with block kinematics (e.g. no penetration and no tension between blocks) and Coulomb friction for sliding along block interfaces. The system of equations (4) is solved for the displacement variables. The final solution to that system is obtained as follows. First, the solution is checked to see how well the constraints are satisfied. If tension or penetration is found along any contact, the constraints are adjusted by selecting new locks and constraining positions and a modified version of **K** and **F** are formed from which a new solution is obtained. This process is repeated until no tension and no penetration is found along all of the block contacts. Hence, the final displacement variables for a given time step are actually obtained by an iterative process.

The simultaneous equations (4) were derived by Shi (1988) by minimizing the total potential energy Π of the block system. The *i*-th row of equation (4) consists of six linear equations

$$\frac{\partial \Pi}{\partial d_{ri}} = 0, \quad r = 1-6 \tag{5}$$

where the d_{ri} are the deformation variables of block i. The total potential energy Π is the summation over all the potential energy sources, i.e. individual stresses and forces. The potential energy of each force or stress and their derivatives are computed separately. The derivatives

$$\frac{\partial^2 \Pi}{\partial d_{ri} \partial d_{sj}}, \quad r,s = 1-6 \tag{6}$$

are the coefficients of the unknowns d_{sj} of the equilibrium equations (4) for variable d_{ri}. All terms of equation (6) form a 6×6 sub-matrix, which is the sub-matrix $\mathbf{K}_{ij}$ in the global equation (4). Equation (6) implies that matrix **K** in equation (4) is symmetric. The derivatives

$$-\frac{\partial \Pi(0)}{\partial d_{ri}}, \quad r = 1-6 \tag{7}$$

are the free terms of equation (5) which are shifted to the right hand side of equation (4). All these terms form a 6×1 sub-matrix, which is added to the sub-matrix $\mathbf{F}_i$.

Shi's thesis(1988) covers the details for forming sub-matrices $\mathbf{K}_{ij}$ and $\mathbf{F}_i$, for elastic stresses, initial stresses, point loads, line loads, volume forces, bolting forces, inertia forces and viscosity forces. Both static and dynamic analyses can be conducted with the DDA method. For static analysis, the velocity of each block in the blocky system at the beginning of each time step is assumed to be zero. On the other hand, in the case of dynamic analysis, the velocity of the blocky system in the current time step is an accumulation of the velocities in the previous time steps.

3. Modeling Water-Block Interaction

A numerical model was developed to study fluid flow in deformable naturally fractured rock masses. The model considers a two-dimensional intact rock mass dissected by a large number of fractures (joints) with variable aperture, length, and orientation. Fluid flow, which occurs when pressure gradients exist, is assumed to be steady, and laminar or turbulent depending on the values of the Reynolds number and the relative roughness of the fracture walls(Louis, 1969). Fluid flow and the rock deformation are fully coupled. Variations in fluid pressure and quantity of fluid result in joint deformation. In turn, joint deformation changes the joint properties, which therefore changes the fluid pressures and the resistance to fluid flow.

3.1 Assumptions

The following assumptions were made when implementing the hydro-mechanical coupling in the DDA program : (a) the fluid is incompressible, (b) the intact rock is impervious, and fluid flow takes place in the joint space only; (c) the rock mass contains a finite

number of joints; (d) the intact rock is linearly elastic; and (e) joint displacements are small relative to the joint dimensions.

In the flow model, the fracture space is idealized as a system of one-dimensional conduits of constant aperture using the approach proposed by Asgian(1988). The *apparent* aperture, b, of a conduit representing a joint depends on the contact between the joint surfaces. The joint can be classified as *closed* or *open* depending on the contact state. Consider, for instance, a closed joint with length, L, and unit width representing the interface between two contacting prismatic blocks of thickness d_1 and d_2 as shown in Fig. 1(a). Let n be the joint surface *contact porosity* (ratio between joint surface open area and total area) of the closed joint which varies between 0 and 1. The joint can be idealized as a portion of void (n) with a uniform aperture, a, and a portion of contacting solid (1-n) with vanishing aperture as shown in Fig. 1(b). The *apparent* aperture, b, of the closed joint is defined as b=a for the portion of void (n).

A representative section of an open joint with length, L, and unit width is shown in Fig. 1(c). The joint represents the open interface between two prismatic blocks of thickness d_1 and d_2 separated by a gap c. The joint can be idealized as one portion of void (n) with aperture, c+a, and another portion of void (1-n) with aperture, c, as shown in Fig. 1(d). The *apparent* aperture, b, of the open joint consists of two components with b_n=c+a for the portion of void (n) and b_{1-n}= c for the other portion of void (1-n).

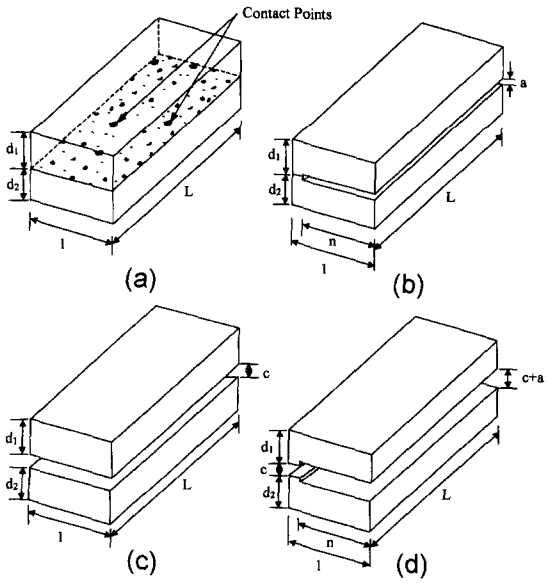

Fig. 1. Joint modeling.
(a) Representative section of closed joint, (b) Idealized section of closed joint, (c) Representative section of open joint, (d) Idealized section of open joint

3.2 Configuration of Water-Block Interaction Model

As shown in Fig. 2, the hydro-mechanical model consists of two major components: the DDA method for the rock mass and the FEM method for joint flow. The initial properties of the joints such as aperture, length, orientation, and boundary conditions from the DDA program are used to compute the piezometric heads and fluid quantities at the joints with a FEM subroutine called RFLOW. The seepage forces acting on the rock blocks are computed from the piezometric heads using a subroutine called WPRESSURE. In the DDA program, joint deformation is computed using the seepage forces. In turn, joint deformation changes the joint properties such as aperture, length, and orientation. A computational loop is followed until the results converge according to a criterion selected by the user.

3.3 Subroutine RFLOW

Louis(1969) showed experimentally that the steady flow of water in a single fracture of constant aperture, b, and surface roughness can be laminar or turbulent depending on the values of the Reynolds number, Re=2bv/v, and the relative roughness, k/D_h, where υ is the average velocity, v the kinematic viscosity of water, k the fracture surface roughness, and D_h the hydraulic diameter of the fracture which is equal to 2b. Louis (1969) also proposed different flow laws relating the friction factor f and the Reynolds number Re which

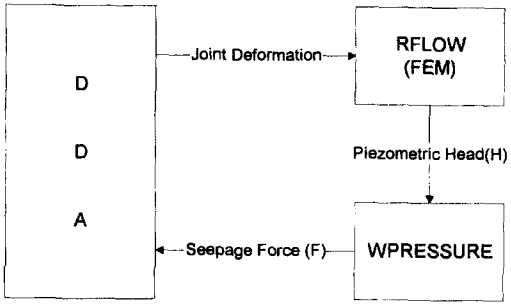

Fig. 2. Water-block interaction model.

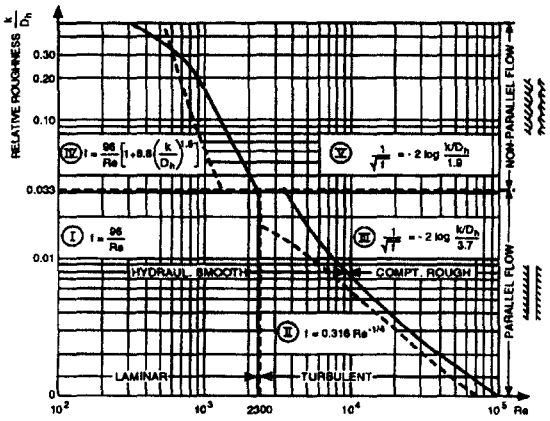

Fig. 3. Compilation of different flow laws and their range of validity for a single fracture. The dashed lines represent mathematical boundaries by Amadei *et al.* (1995) and the solid lines the boundaries determined experimentally by Louis (1969).

apply in different regions of the (Re, k/D_h) space. Fig. 3 shows five such regions I-V, their corresponding mathematical boundaries and the experimental boundaries proposed by Louis(1969).

For parallel flow, and as shown by Amadei *et al.* (1995), the mathematical boundary between turbulent hydraulic smooth flow (region II) and turbulent completely rough flow (III) in Fig. 3 can be expressed as

$$Re = 2.553\left[\log\left(\frac{k/D_h}{3.7}\right)\right]^8 \tag{8}$$

For non-parallel flow, and as shown by Amadei *et al.* (1995), the mathematical boundary between laminar flow (region IV) and turbulent flow (region V) in Fig. 3 can be expressed as

$$Re = 384[1+8.8(k/D_h)^{1.5}]\left[\log\left(\frac{k/D_h}{1.9}\right)\right]^2 \tag{9}$$

The mathematical boundaries defined by equations (8) and (9) are shown as dashed lines in Fig. 3. These mathematical boundaries were used in the non-linear model presented below.

According to Bernoulli's theorem for ideal frictionless incompressible fluids, the sum of the *pressure head*, $h_p = p/\gamma_w$, *elevation head*, $h_e = z$ and *velocity head*, $h_v = v^2/2g$, is constant at every point of the fluid, e.g.

$$\frac{p}{\gamma_w}+z+\frac{v^2}{2g}=H+h_v=\text{constant}=H_t \tag{10}$$

where p is the pressure, z the elevation, v the average velocity, H the piezometric head ($=h_p+h_e$), and H_t the total head.

In the steady flow of water in a single fracture of constant aperture, b, and length, L, the total head loss, ΔH_t, (also equal to the piezometric head loss, ΔH) takes place due to the viscous resistance within the fracture. As shown by Louis(1969), the average velocity, v, and the gradient of piezometric head, $i = \Delta H/L$, (also equal to the gradient of total head, $\Delta H_t/L$) for each hydraulic region of Fig. 3 can be written as follows

$$v = Ki^{\alpha} = K\left(\frac{\Delta H}{L}\right)^{\alpha} \tag{11}$$

where ΔH is the piezometric head loss. Values of the hydraulic conductivity, K, and the exponent, α, for each flow region of Fig. 3 are reported in Table 1. For each hydraulic region, the element discharge, Q, and the piezometric gradient, $i = \Delta H/L$, are such that

$$Q = vb = Kb\left(\frac{\Delta H}{L}\right)^{\alpha} \tag{12}$$

Equation (12) can be rewritten as

$$Q = T\Delta H \quad \text{with} \quad T = \frac{Kb}{L^{\alpha}}\Delta H^{\alpha-1} \tag{13}$$

where T is the so-called fracture transmissivity.

Equation (13) is then modified depending on the contact state (closed or open) between the joint sur-

Table 1. Expression of hydraulic conductivity and degree of non-linearity for the different hydraulic regions of Fig. 3 (after Louis(1969))

Hydraulic Region	Hydraulic Conductivity (K)	Exponent (α)	Flow Condition
I	$K_I = \frac{g \cdot b^2}{12\nu}$	1.0	Laminar
II	$K_{II} = \frac{1}{b}\left[\frac{g}{0.079}\left(\frac{2}{\nu}\right)^{0.25} \cdot b^3\right]^{4/7}$	4/7	Turbulent
III	$K_{III} = \sqrt[4]{g}\ \log\left[\frac{3.7}{k/D_h}\right]\sqrt{b}$	0.5	Turbulent
IV	$K_{IV} = \frac{gb^2}{12\nu[1+8.8(k/D_h)^{1.5}]}$	1.0	Laminar
V	$K_V = \sqrt[4]{g}\ \log\left[\frac{1.9}{k/D_h}\right]\sqrt{b}$	0.5	Turbulent

faces. For a closed joint (Fig. 1(b)), the element discharge, Q, is defined as

$$Q = T\Delta H \quad \text{with} \quad T = n\frac{Kb}{L^{\alpha}}\Delta H^{\alpha-1} \tag{14}$$

For an open joint (Fig. 1(d)), the element discharge, Q, is defined as

$$Q = T\Delta H \quad \text{with} \quad T = n\frac{K_n b_n}{L^{a_n}}\Delta H^{a_n-1} + (1-n)\frac{K_{1-n} b_{1-n}}{L^{a_{1-n}}}\Delta H^{a_{1-n}-1} \tag{15}$$

where K_n and α_n are respectively the hydraulic conductivity and exponent for one portion of void (n) with apparent aperture b_n=c+a. Likewise, K_{1-n} and α_{1-n} are respectively the hydraulic conductivity and exponent for the other portion of void (1-n) with apparent aperture b_{1-n}=c.

Consider now a single planar joint element, i, of length L^i and constant aperture b^i as shown in Fig. 4(a). Equation (13) can be used to compute the discharge through the joint element in terms of the piezometric head loss between its two end nodes defined here as j and k. The discharge at node k, Q^i_k, and the discharge at node j, Q^i_j, are equal to

$$Q^i_k = T^i\Delta H^i = T^i(H^i_k - H^i_j)$$

$$Q^i_j = -T^i\Delta H^i = -T^i(H^i_k - H^i_j) \tag{17}$$

These two equations can be rewritten in matrix form as follows

$$\begin{Bmatrix} Q^i_k \\ Q^i_j \end{Bmatrix} = T^i\begin{bmatrix} 1 & -1 \\ -1 & 1 \end{bmatrix}\begin{Bmatrix} H^i_k \\ H^i_j \end{Bmatrix} \quad \text{or} \quad \mathbf{Q}^i = \mathbf{T}^i\mathbf{H}^i \tag{17}$$

where $\mathbf{Q}^i$ is the element nodal discharge vector, $\mathbf{T}^i$ the element characteristic matrix, and $\mathbf{H}^i$ the element nodal piezometric head vector.

So far, the elements in the network have been considered individually, and expressions giving the discharges in terms of the nodal piezometric heads have been developed. For a complete joint network, however, the interaction between the different elements needs to be taken into account. This implies that there must exist equilibrium at any given node of the network between the discharges of the elements connected to the node, including any inflow or outflow at that node. Consider a simplified model of a fracture network below a dam as shown in Fig. 4(b). The quantity C_j is the inflow (C_1 and C_3) or outflow (C_5 and C_7) at any node j. In general, any C_j will be positive for inflow (C_1 and C_3) and negative for outflow (C_5 and C_7). Equilibrium at any node means that the sum of the discharges of the elements connected to the node equals the inflow or outflow at that node. For any node j, the equilibrium equation can be expressed as follows:

$$\sum_i Q^i_j = C_j \tag{18}$$

where the summation runs over all elements connected to node j. By repeating the procedure for all n nodes, and using equations (17) and (18), a system of equations can be derived e.g.

$$\begin{bmatrix} T_{11} & T_{12} & \cdots & T_{1n} \\ T_{21} & T_{22} & \cdots & T_{2n} \\ \vdots & \vdots & \ddots & \vdots \\ T_{n1} & T_{n2} & \cdots & T_{nn} \end{bmatrix}\begin{Bmatrix} H_1 \\ H_2 \\ \vdots \\ H_n \end{Bmatrix} = \begin{Bmatrix} C_1 \\ C_2 \\ \vdots \\ C_n \end{Bmatrix} \quad \text{or} \quad \mathbf{TH} = \mathbf{C} \tag{19}$$

where $\mathbf{T}$ is the network characteristic matrix, $\mathbf{H}$ is the

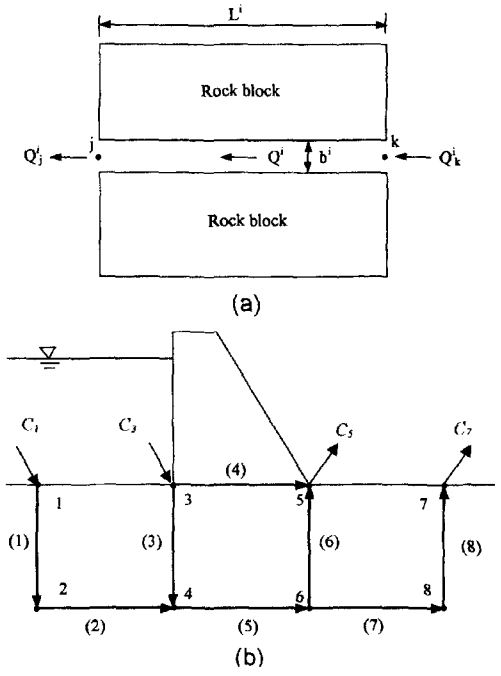

Fig. 4. Construction of total system of equations. (a) Single joint element, (b) Joint network

network piezometric head vector, and **C** is the network flow vector. Before the total system of equations (19) can be solved, it is necessary to introduce the boundary conditions for the network nodes. The boundary conditions at a given node j can be of two types; specified piezometric head (H_j) or specified flow (C_j).

The total system of equations (19) is a non-linear system due to the fact that **T** depends on **H**. However, it can be solved by successive iterations. First, for each joint element, flow is assumed to be laminar with (α=1.0 and $K=K_I$ or K_{IV} and an initial value for the nodal piezometric head, H_{ini}, is assumed for each node. The fracture transmissivity, T, is computed using equation (14) or (15) for each joint element, and the total system of equations (19) is formed using equations (17) and (18). The total system of equations is solved by the Gauss elimination method to obtain a new value of the nodal piezometric head, H_{new}, for each node. The velocity, υ, defined by equation (11) and the Reynolds number, $Re=2b\upsilon/\nu$, are calculated for each joint element using the new value of the nodal heads. Using Fig. 3, the values of Re and the relative roughness, k/D_h, determine if the flow in each joint element is laminar or turbulent. If the flow is laminar, α and K remain the same. If, on the other hand, turbulent flow develops, new values of α and K are selected using Fig. 3 and Table 1 for each joint element, and a new initial value for the nodal piezometric head is assumed with $H_{ini}=H_{new}$ for each node in the next iteration. Then, using equation (14) or (15), a new fracture transmissivity, T, is computed for each element, and a new total system of equations is formed. The total system of equations is solved to obtain a new value of the nodal piezometric head, H_{new}, for each node. The process is repeated until, for two successive steps, α and K remain the same and $|H_{new}-H_{ini}|/H_{ini}$ is below a minimum tolerance specified by the user.

As a validity check of the RFLOW subroutine, a comparison was made with the experimental work reported by Grenoble(1989), who constructed a physical laboratory model to simulate two-dimensional flow through a jointed rock mass(Kim, 1988).

3.4 Subroutine WPRESSURE

A new algorithm for computing seepage forces acting on rock blocks from the nodal piezometric heads was developed. The fluid pressure acting on the rock blocks can be computed from the values of the pressure heads at those nodes defining the blocks. The fluid pressures are transformed as point loads along the sides of each rock block. Then, the point loads are given as boundary conditions in the Discontinuous Deformation Analysis. Using this approach, there is no need to artificially regulate the deformations of the joints as in other methods. Therefore, the rock blocks can deform freely according to block system kinematics.

As a validity check of the WPRESSURE subroutine in the DDA program, the problem of the opening of a crack (joint) in an infinite domain subjected to an internal pressure was considered and compared with an analytical solution(Kim, 1998).

4. Effect of Water Level on Tunnel Stability

The excavation of a (half) circular tunnel is considered as a numerical example. The tunnel has a diameter, D, of 10 m and is located at a depth of 409.6 m below the surface. The water level varies between 100 and 500 m above the center of the tunnel. The domain of analysis is 5D (50 m) wide and 4D plus tunnel height (46.71 m) high. A vertical compressive stress of 10 MPa is applied on the top boundary of the domain (to simulate the load associated with 384.6 m of rock) and no lateral deformation is allowed. The intact rock has a unit weight of 26 KN/m^3, a Young's modulus of 3.6 GPa, and a Poisson's ratio of 0.2. The joints have a spacing of 4 m, an initial aperture of 0.01 mm, a normal stiffness of 36 GN/m, a friction angle of 35° and a cohesion of 0.5 MPa. No reinforcement is applied in this example. As boundary conditions, only elevation heads (zero pressure heads) were applied on the nodes along the excavated surface of the tunnel.

Without water the settlement of the tunnel roof was found to be equal to 165.2 mm (Table 2). The tunnel roof deforms but does not collapse as shown in Fig. 5(a). As the water level increases, the tunnel roof settlement increases resulting in complete collapse of the tunnel (see Table 2 and Figs. 5(b)-(f)).

5. Conclusion

The hydro-mechanical coupling algorithm was im-

Table 2. Effect of water level on the stability of the tunnel in Fig. 5

Water Level (m)	Roof Settlement (mm)
0	165.2
100	237.6
200	706.4
300	1632.8
400	2088.2
500	4514.0

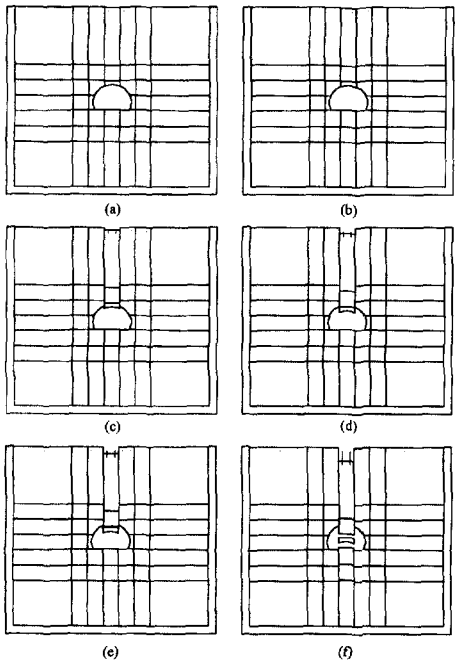

Fig. 5. Effect of water level on tunnel stability. (a) No water, (b) W.L.: 100 m, (c) W.L.: 200 m, (d) W.L.: 300 m, (e) W.L.: 400 m, (f) W.L.: 500 m

plemented into the original DDA program of Shi (1988) and modified by Lin(1995). The algorithm includes hydro-mechanical coupling between rock blocks and water flow in fractures.

The hydro-mechanical coupling algorithm is very important in rock engineering problems were seepage takes place in natural fractures and joints.

Seepage forces and water pressure can be controlling factors in rock mass stability as illustrated in the tunnel example presented in this paper.

The new algorithm is limited to steady state flow and needs to be modified to include transient flow phenomena.

Reference

1. Amadei, B., Carlier, J. F., Illangasekare, T. H., 1995, Effects of turbulence on fracture flow and advective transport of solutes. *Int. J. Rock Mech. Min. Sci. & Geomech. Abs.*, **32**, pp. 343-356.
2. Asgian, M. I., 1988, *A numerical study of fluid flow in deformable, naturally fractured reserviors*. Ph.D. thesis, University of Minnesota.
3. Goodman, R. E., 1966, On the distrubution of stresses around circular tunnels in non-homogeneous rocks, *Proceeding of 1st International Congress on Rock Mechanics, Lisbon*.
4. Goodman, R. E., 1968, Effects of joints on the strength of tunnels, *Technical Report No. 5*, Omaha District, U.S. Army CE, Omaha.
5. Grenoble, B. A., 1989, *Influence of geology on seepage and uplift in concrete gravity dam foundations*. Ph.D. thesis, University of Colorado at Boulder, Colo.
6. Ke, T. C. and Goodman, R. E., 1994, Discontinuous deformation analysis and 'the artificial joint concept'. *Proceedings of 1st NARMS*, UT, Austin, pp. 599-606.
7. Kim, Y.I., 1998, *Modeling the Effect of Water, Excavation Sequence and Reinforcement on the Response of Blocky Rock Masses*, Ph.D. thesis, Univ. of Colorado at Boulder.
8. Lin, C. T., 1995, *Extensions to the discontinuous deformation analysis for jointed rock masses and other block systems*. Ph.D. thesis, University of Colorado at Boulder, Colo.
9. Louis, C., 1969, A study of groundwater flow in jointed rock and its influence on the stability of rock masses. Imperial College, Rock Mechanics Research Report No. 10.
10. Ohnishi, Y., 1997, *Proc. of the Second International Conference on Analysis of Discontinuous Deformation*, Kyoto, Japan.
11. Salami, M. R. and Banks, D., 1996, Discontinuous deformation analysis (DDA) and simulations of discontinuous media. *Proc. of the First International Forum on Discontinuous Deformation Analysis (DDA) and Simulations of Discontinuous Media*, Berkeley, Calif.
12. Shi, G. H., 1988, *Discontinuous deformation analysis: a new numerical model for the statics and dynamics of block systems*. Ph.D. thesis, University of California, Berkeley, Calif.
13. Shi, G. H., and Goodman, R. E., 1989, Generalization of two-dimensional discontinuous deformation analysis for forward modeling. *International Journal for Numerical and Analytical Methods in Geomechanics*, **13**, pp. 359-380.
14. Shi, G. H., 1990, Forward and backward dis-

continuous deformation analyses of rock systems. *Proceedings of International Conference of Rock Joints*, Leon, Norway, pp. 731-743.
15. Sneddon, I. N. and Lowengrub, M., 1969, *Crack problems in the classical theory of elasticity.* Joh Wiley & Sons, Inc., New York.
16. Yeung, M. R. and Klein, S. J., 1994, Application of the discontinuous deformation analysis to the evaluation of rock reinforcement for tunnel stabilization. *Proceedings of 1st NARMS*, UT, Austin, pp. 607-614.